Journal of Rock Mechanics and Geotechnical Engineering 8 (2016) 789–804

Contents lists available at ScienceDirect

Journal of Rock Mechanics and Geotechnical Engineering

journal homepage: www.rockgeotech.org

Full Length Article

Fault activation and induced seismicity in geological carbon storage – Lessons learned from recent modeling studies

Jonny Rutqvist [a,*], Antonio P. Rinaldi [a,b], Frederic Cappa [a,c], Pierre Jeanne [a], Alberto Mazzoldi [a,d], Luca Urpi [b], Yves Guglielmi [a], Victor Vilarrasa [a,e]

[a] Energy Geosciences Division, Lawrence Berkeley National Laboratory (LBNL), Berkeley, USA
[b] Swiss Seismological Service, Swiss Federal Institute of Technology (ETHZ), Zürich, Switzerland
[c] GéoAzur, University of Nice Sophia-Antipolis, Côte d'Azur Observatory, Nice, France
[d] UMSNH-IIM, Instituto de Investigaciones en Ciencias de la Tierra, Morelia, Mexico
[e] Institute of Environmental Assessment and Water Research (IDAEA), Spanish Council for Scientific Research (CSIC), Barcelona, Spain

ARTICLE INFO

Article history:
Received 11 July 2016
Received in revised form
6 September 2016
Accepted 10 September 2016
Available online 20 September 2016

Keywords:
Carbon dioxide (CO_2) injection
Fault rupture
Induced seismicity
Ground motion
Leakage
Modeling

ABSTRACT

In the light of current concerns related to induced seismicity associated with geological carbon sequestration (GCS), this paper summarizes lessons learned from recent modeling studies on fault activation, induced seismicity, and potential for leakage associated with deep underground carbon dioxide (CO_2) injection. Model simulations demonstrate that seismic events large enough to be felt by humans require brittle fault properties and continuous fault permeability allowing pressure to be distributed over a large fault patch to be ruptured at once. Heterogeneous fault properties, which are commonly encountered in faults intersecting multilayered shale/sandstone sequences, effectively reduce the likelihood of inducing felt seismicity and also effectively impede upward CO_2 leakage. A number of simulations show that even a sizable seismic event that could be felt may not be capable of opening a new flow path across the entire thickness of an overlying caprock and it is very unlikely to cross a system of multiple overlying caprock units. Site-specific model simulations of the In Salah CO_2 storage demonstration site showed that deep fractured zone responses and associated microseismicity occurred in the brittle fractured sandstone reservoir, but at a very substantial reservoir overpressure close to the magnitude of the least principal stress. We conclude by emphasizing the importance of site investigation to characterize rock properties and if at all possible to avoid brittle rock such as proximity of crystalline basement or sites in hard and brittle sedimentary sequences that are more prone to injection-induced seismicity and permanent damage.

1. Introduction

Fault activation and induced seismicity associated with geological carbon sequestration (GCS) have in recent years become an intensively studied topic (Rutqvist, 2012). Concerns are mostly related to the potential for triggering notable (felt) seismic events and how such events could impact the long-term integrity of a carbon dioxide (CO_2) repository, as well as how they could impact the public perception of GCS (Fig. 1). The issue of induced seismicity has received broader attention among GCS stakeholders since 2012 when two high-profile publications appeared. First, in a study requested by the U.S. Government, The National Research Council (2012) concluded that projects involving large net volume of fluid injection and/or extraction of over long periods of time (such as GCS) may have the potential to induce large seismic events, though there was not sufficient information for understanding this potential for GCS, because no large-scale projects were yet in operation. Second, Zoback and Gorelick (2012) warned for the high probability that earthquakes would be triggered by injection of large volumes of CO_2 into the brittle rocks commonly found in continental interiors. They concluded that large-scale GCS would be a risky and likely unsuccessful strategy for significantly reducing greenhouse gas emissions to the atmosphere, because even small- to moderate-sized earthquakes could threaten the seal integrity of CO_2 repositories. These views have since been debated and

* Corresponding author.
E-mail address: Jrutqvist@lbl.gov (J. Rutqvist).
Peer review under responsibility of Institute of Rock and Soil Mechanics, Chinese Academy of Sciences.

http://dx.doi.org/10.1016/j.jrmge.2016.09.001

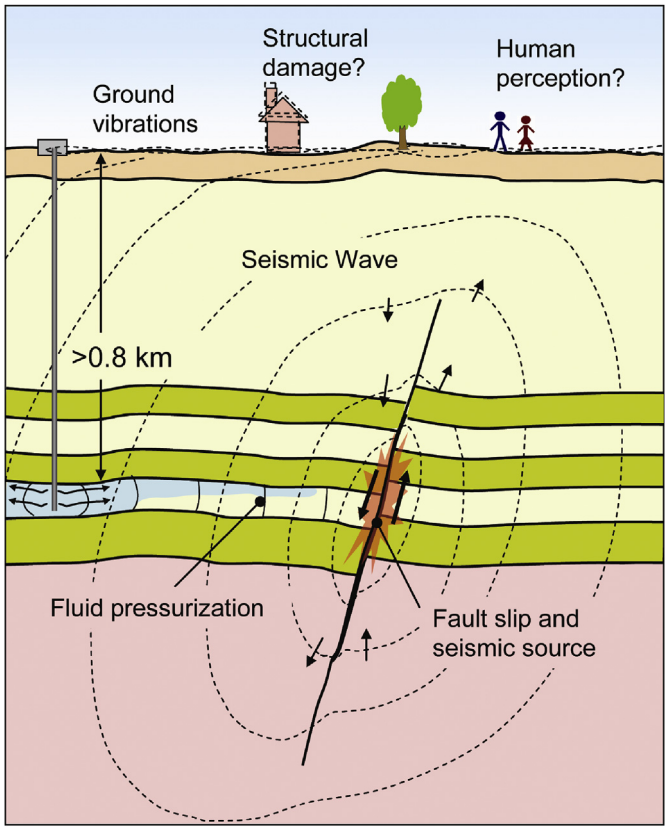

Fig. 1. Schematic of CO_2-injection-induced fault reactivation and potential impact on surface structures and human perception (Rutqvist et al., 2014).

questioned by some other researchers such as Juanes et al. (2012) and Vilarrasa and Carrera (2015).

In their article, Zoback and Gorelick (2012) mentioned reservoir-induced earthquakes associated with dam construction and water-reservoir impoundment as a good analog for the seismicity that potentially could be induced by large-scale CO_2 injection, because both activities cause pressure changes that act over large areas and are persistent for long periods. They also listed a number of recent small-to-moderate seismic events in the U.S. that seem to have been triggered by deep waste-water injection, referring to the critically stressed nature of the Earth's crust, which suggests that a subset of preexisting faults in the crust is potentially active in the current stress field almost everywhere in the continental interior (Zoback and Zoback, 1989). Because of the critically stressed nature of the crust, fluid injection in deep wells may induce earthquakes when injection increases the pore pressure in the vicinity of potentially active faults.

Since these two publications in 2012, concerns have been further amplified by the recent surge of injection-induced seismicity in the mid-continental U.S. as a result of waste-water injection (Ellsworth, 2013; Keranen et al., 2014; McGarr et al., 2015; Weingarten et al., 2015). In many of these cases, injected waste-water fluids seem to have communicated from the target formation to greater depth along preexisting faults, as evidenced by earthquake locations in the crystalline basement (Horton, 2012; Zhang et al., 2013; Verdon, 2014; Hornbach et al., 2015; McGarr et al., 2015). Vilarrasa and Carrera (2015) suggested that this higher rate of induced seismicity in the crystalline basement is a result of the deviatoric stresses that tend to be higher in the stiff basement rocks compared to the softer overlying sediments. Highlighted herein is also the critical importance of brittle-versus-ductile rock properties that could be decisive on whether fault activation induced by deep underground CO_2 injection could result in a felt seismic event and permanent damage to the CO_2 repository seal.

In the light of these concerns, this paper summarizes lessons learned from recently published modeling studies on fault reactivation associated with CO_2 injection into deep sedimentary formations. The model simulations were conducted using a coupled multiphase fluid flow and geomechanics numerical model (Rutqvist, 2011) applying deterministic modeling of a fault with evolving frictional coefficient that enables the simulation of sudden (seismic) fault rupture. In some cases, the modeling was extended to include the entire chain of processes of CO_2 injection, reservoir pressurization, dynamic fault-reactivation-induced seismic source, wave propagation, and ground motion. Finally, we summarize the results and lessons learned from modeling of injection-induced deep fracture zone responses at the In Salah CO_2 storage site, and conclude with recommendations to minimize the potential of induced seismicity and damaging geomechanical changes during a GCS operation.

2. Lessons learned from generic fault activation studies

In this section, we summarize lessons learned from generic (not site-specific) modeling studies on potential fault activation, induced seismicity and leakage associated with CO_2 injection into deep underground sedimentary formations. The model simulations were conducted using the TOUGH-FLAC simulator (Rutqvist et al., 2002; Rutqvist, 2011) which is based on linking the TOUGH2 finite-volume code for the simulation of multiphase fluid flow (Pruess et al., 2012) with the FLAC3D finite-difference code for the simulation of geomechanics (Itasca Consulting Group, 2011). The TOUGH-FLAC simulator was first applied for deterministic modeling of fault activation in Rutqvist et al. (2007) and in the modeling of the 1960s Matsushiro earthquake swarm by Cappa et al. (2009). Later, Cappa and Rutqvist (2011a) further tested the TOUGH-FLAC simulator with the deterministic fault activation model using different fault mechanical approaches, including representation of faults by slip interfaces or finite-thickness elements with isotropic or anisotropic elastoplastic constitutive models. Cappa and Rutqvist (2011a) then utilized the finite-thickness fault element approach coupled with a strain-permeability model to show the important role of shear-enhanced permeability in propagating fault instability and permeability enhancement through the overlying caprock. The TOUGH-FLAC simulator with such fault activation modeling approach has since been applied in a number of studies, in which the constitutive models for fault permeability and friction have been further developed, including slip-weakening and slip-rate dependent friction. In the following subsections, the main findings and lessons learned from these generic simulation studies are summarized.

2.1. Simulation of a felt seismic event on a major fault

Results from Cappa and Rutqvist (2011b) are presented as an example to illustrate what it takes to create a seismic event that might be felt by humans on the ground surface. Fig. 2a shows the model geometry and Fig. 2b the fault friction model. Details on the modeling input including material properties can be found in Cappa and Rutqvist (2011b). A strain-softening fault constitutive mechanical model was used as it enables modeling of sudden (seismic) fault slip. Using this approach in a quasi-static mechanical analysis in FLAC3D, discrete events of fault activation were modeled and the associated seismic moment magnitude was estimated

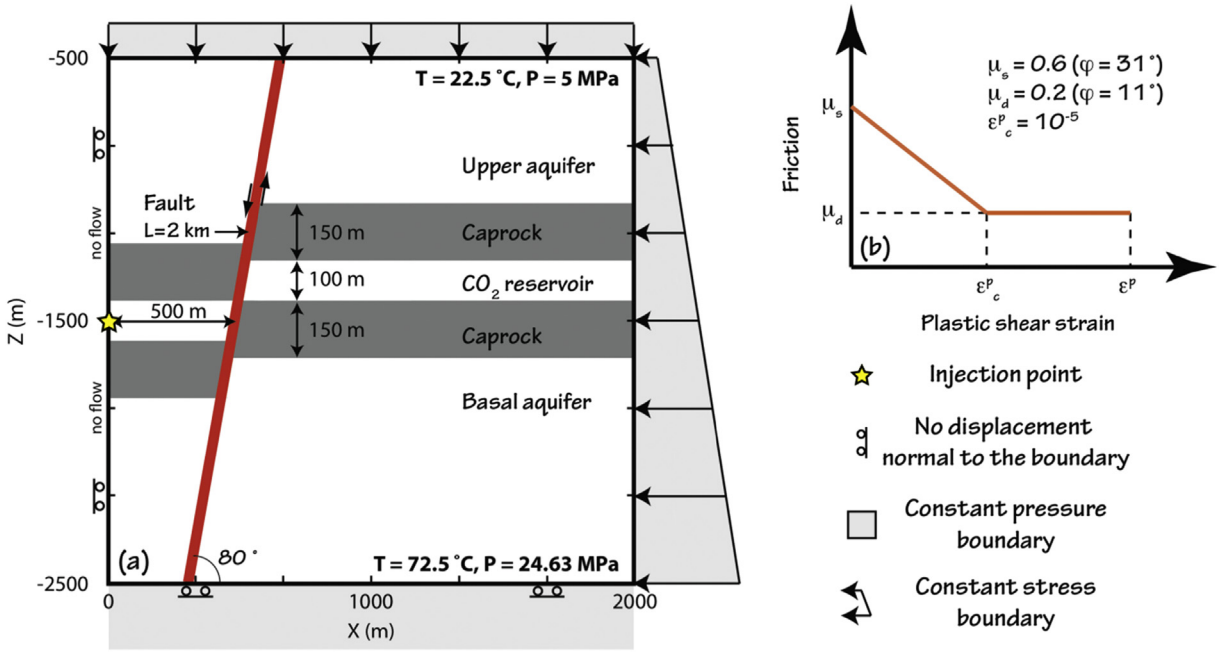

Fig. 2. (a) Numerical model geometry and initial conditions. We assumed a normal fault with a 125 m offset through a 100 m thick reservoir bounded at the top and the bottom by a 150 m thick caprock. (b) A plastic shear strain-weakening friction law that governs the propagation of rupture along the fault zone (modified from Cappa and Rutqvist, 2011b).

through seismology relationships by Kanamori and Anderson (1975) and Hanks and Kanamori (1979). That is, the co-seismic (unstable) slip that occurs in the mechanical calculation from one fluid-flow time step to another was used to calculate the seismic moment and moment magnitude from the product of the rupture area, the average shear displacement, and the rock shear modulus.

One of the key parameters in the modeling of fault activation and associated rupture size is the coefficient of friction and its evolution with shear slip. Most commonly in these generic modeling studies, a slip-weakening model is applied, in which the coefficient of friction drops from a peak (static, μ_s) value of 0.6 to a residual (dynamic, μ_d) value of 0.2 over some pre-defined (very small) slip displacement. In most cases, this slip-weakening behavior is modeled using the finite-thickness fault elements, anisotropic Mohr-Coulomb plasticity, with strain-softening coefficient of friction over a certain critical shear strain (ε_c^P in Fig. 2b). As discussed in several papers (e.g. Rutqvist et al., 2014), these values of coefficient of friction adopted for input to the numerical model are uncertain and can be considered as one set of possible parameters displaying a relatively large difference between peak and residual frictions designed for generating a reasonable injection-induced seismic event for these generic fault activation studies.

Fig. 3 shows the simulation results of an injection-induced $M_w = 3.4$ seismic event that occurred as a result of fault activation at 1.5 km depth (Cappa and Rutqvist, 2011b). This modeling case considered a fault with a pre-injection shear displacement offset (throw) of 125 m, which provides an unfavorable case where fluid pressure builds up only on one side of that fault. Such one-sided pressure buildup creates increased shear stress across the fault along with reduced normal effective stress and fault shear strength (Fig. 3b). Fig. 3a shows that after about 90 days of injection, the fault reactivates with about 8 cm shear slip. A fault section of 385 m was instantaneously ruptured once the reservoir overpressure exceeded 10 MPa (Fig. 3b and d). A $M_w = 3.4$ seismic event is equivalent to the maximum magnitude of the earthquakes that were induced at the well-known Basel geothermal project, which were felt by the local population and caused the closure of the project due to public opposition (Häring et al., 2008). In Fig. 4, the results for simulations at different initial stress states (ratio between horizontal and vertical stresses being $\sigma_h/\sigma_v = 0.6$, 0.7 and 0.8) were related to other field data from both natural and injection-induced seismicity. Fig. 4 shows that an event with magnitude of 4 would require a source radius in the order of 1 km. Overall, the simulation results in Cappa and Rutqvist (2011b) showed that the size of the rupture area, and consequently, the earthquake magnitude and energy are strongly dependent on the initial horizontal-to-vertical stress ratio and also somewhat dependent on fault permeability. That is, if the fault permeability is higher, the seismic events induced tended to be slightly larger. We also note that even in the case of the highest shear stress, the modeled fault is still not critically stressed on the verge of shear failure, meaning that a certain overpressure is required to trigger fault activation and seismicity. The fact that seismicity was triggered in these cases is a result of the slip-weakening (strain-softening) fault model, which assumes brittle fault behavior in these deep sedimentary formations.

2.2. Maximum seismic moment magnitudes for undetectable faults

Mazzoldi et al. (2012) discussed the possibility of bounding the maximum seismic magnitude that could occur for faults that might have gone undetected during the site characterization process. An undetected fault was envisioned as a fault with a shear offset (throw) of less than 10 m, because such a fault might not be clearly visible using the current industry-standard surface seismic survey. Moreover, as described in Mazzoldi et al. (2012), based on empirical fault geometry data, a fault with 10 m throw could be expected to be less than 1 km long. Therefore, the case of a 1 km long fault having a small offset was analyzed and exposed to reservoir pressurization at a depth of 1.5 km (Fig. 5a). Compared to the case described above, here the initial fault shear offset (throw) is small compared to the thickness of the reservoir, and therefore the reservoir is not completely bounded from hydraulic viewpoint. The

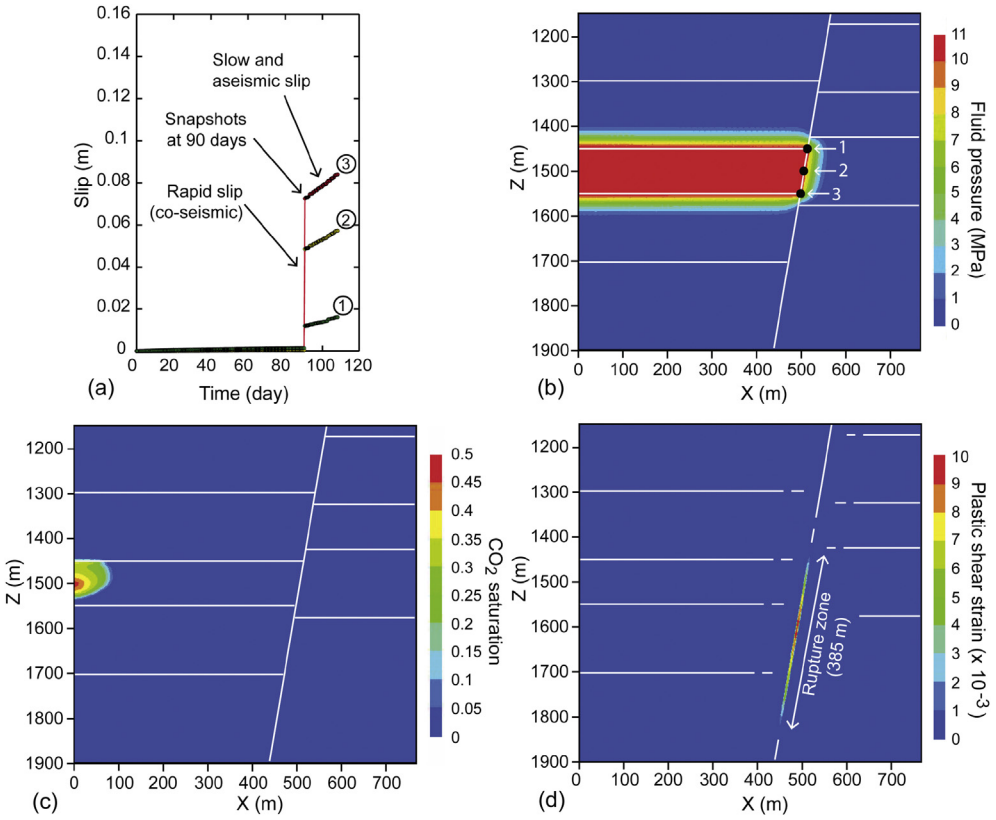

Fig. 3. (a) Fault slip versus time at three points located at the top (1), middle (2) and bottom (3) of the reservoir, respectively (see Fig. 3b for the location). Snapshots of changes (relative to the initial state) in (b) fluid pressure, (c) CO_2 saturation, and (d) plastic shear strain at the end of the sudden slip event (after 90 days of CO_2 injection). Black circles in (b) are control points used to compare the simulation results (modified from Cappa and Rutqvist, 2011b).

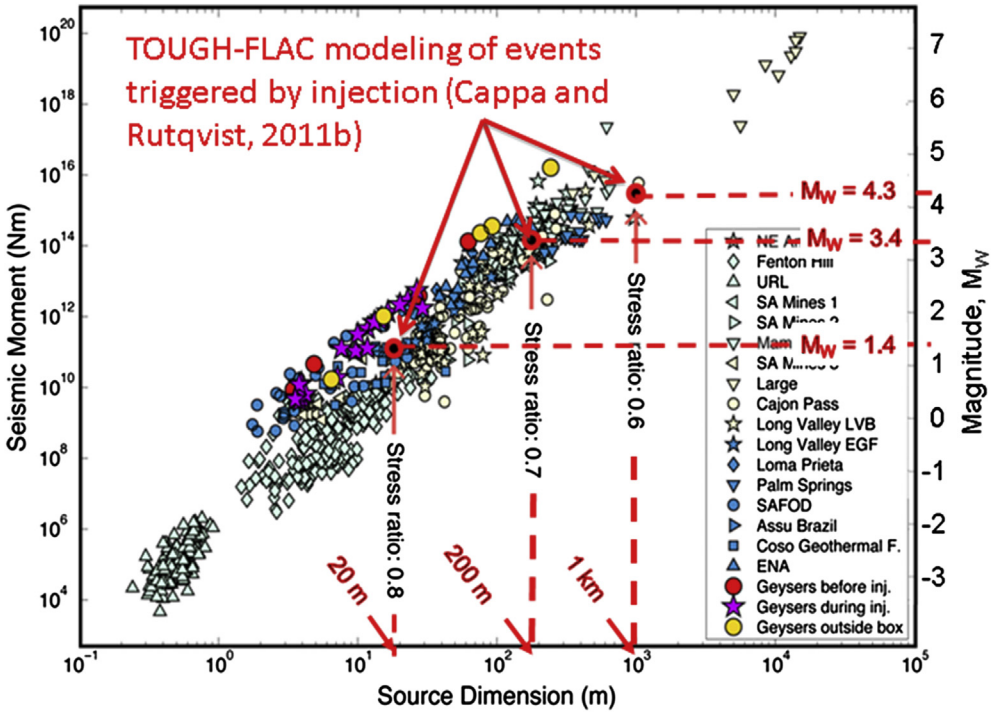

Fig. 4. Seismic scaling relationship after Viegas et al. (2010): source dimension (radius), seismic moment and magnitude. Red and black circles correspond to simulation results of CO_2 injection-induced fault reactivation by Cappa and Rutqvist (2011b).

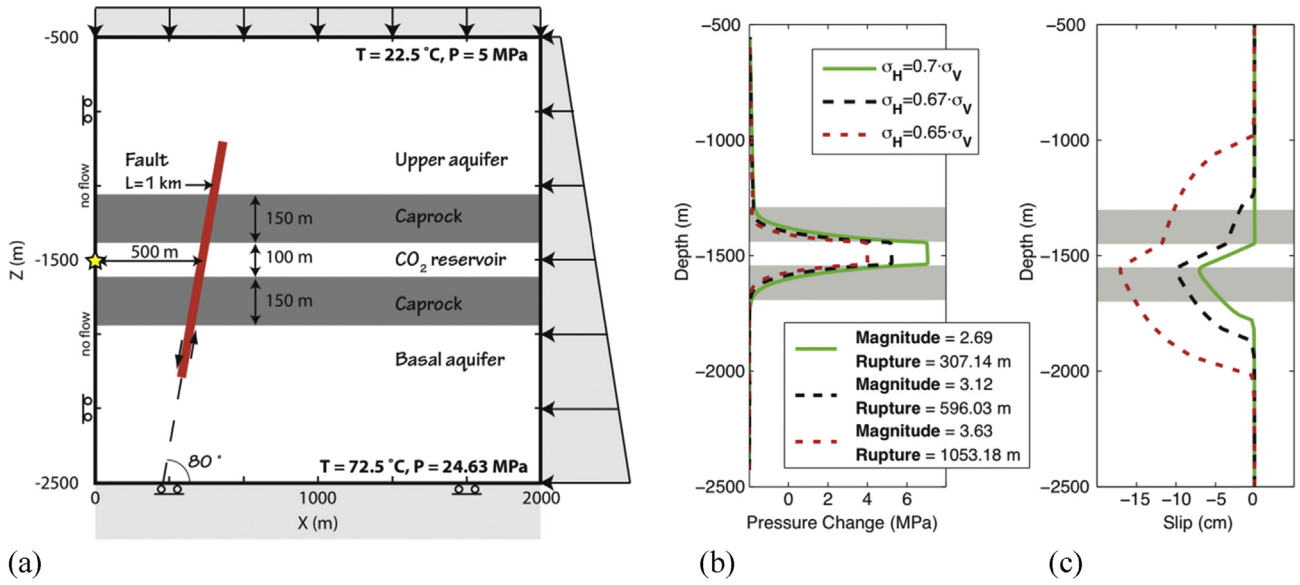

Fig. 5. Results of simulations analyzing the response of fault slip to changes in value of stress at the fault surface in the case of a minor (1 km long) fault (Mazzoldi et al., 2012), considering stress ratios equal to 0.7, 0.67 and 0.65. Highest resulting values of moment magnitude and rupture length are for faults exposed to stress nearest to instability. (a) Model geometry, (b) pressure change at rupture, and (c) co-seismic slip for the three different stress ratios considered.

fault will act as a flow barrier only if its cross-fault permeability is small compared to that of the reservoir.

A permeability distribution along the fault was adopted based on geological evidence in this TOUGH-FLAC numerical modeling. For example, permeability of the fault section within the caprock was set to be orders of magnitude smaller than that of the fault section within the sandstone. Simulations showed that only in the case of fault permeability at least two orders of magnitude lower than that of the sandstone aquifer, it is possible to obtain a sufficient absolute pressure increase for the given injection rate and cross-fault pressure gradient with associated cross-fault shear stress that could trigger fault reactivation. In the reference case, the fault permeability $k_{\text{F-Aq}} = 10^{-15}$ m^2 in the fault gouge of the sandstone layers and $k_{\text{F-Cap}} = 10^{-16}$ m^2 in the fault gouge of the shale.

For a horizontal-to-vertical stress ratio of 0.7, the fault rupture was about 310 m extending through the lower caprock, but not through the upper one, because of the permeability differences in the fault zone portion within the sandstone and the caprock, and a difference in induced shear stress in the upper and lower caprocks. The calculated moment magnitude M_w was about 2.7. However, when the stress ratio was reduced to 0.65, the fault ruptured in a self-propagating mode, and the entire 1 km long fault ruptured (Fig. 5b and c). The magnitude M_w was estimated to be about 3.6 in this case. Thus, when the fault is closer to being critically stressed for shear failure (in this case, lowering the horizontal-to-vertical stress ratio as a way of considering different values of horizontal stresses, σ_2 and σ_3), the fault rupture could self-propagate further outside the pressurized zone, and the rupture was limited only by the length of the fault. The reason that the fault rupture could self-propagate was that the residual shear strength of the fault (for a residual coefficient of friction μ_d of 0.2) was close to the prevailing shear stress across the fault. A reservoir overpressure of about 4 MPa was required to activate the fault at peak shear strength (for a peak coefficient of friction μ_s of 0.47), but, because of the strain-softening during shear rupture to a residual shear strength value close to the prevailing shear stress, the fault rupture could self-propagate outside the pressurized zone.

2.3. Dynamic fault-activation response

Cappa and Rutqvist (2012) extended the previous quasi-static analysis by Cappa and Rutqvist (2011b) to include fully dynamic analysis of fault activation and seismic wave propagation generated by the rupture. The case shown in Fig. 2a was considered with an offset fault bounding the reservoir and a horizontal-to-vertical stress ratio of 0.7. In this case, however, the depth was not 1.5 km as shown in Fig. 2a, but was reduced to 1 km so that the top of the model represents the ground surface. The modeling in Cappa and Rutqvist (2012) involved a transition between the initial quasi-static phase and the dynamic phase occurring during rupture. Moreover, for this dynamic analysis, a refined mesh was used with element sizes of 0.25 m along the rupture zone in order to resolve the weakening process over the nucleation zone and to avoid mesh-induced artificial reflections.

Fig. 6 presents a set of results related to the reactivation of the fault by pressurization of the reservoir at 1 km. For the assumed system and injection rate, the simulations showed that after 40 days of injection, a dynamic fault rupture nucleates at the base of the CO_2 reservoir. At the initiation of the fault rupture, the fluid pressure had increased by about 7.5 MPa, i.e. achieving a total fluid pressure of 17.5 MPa, which is a few megapascals higher than the local initial minimum principal stress at 1 km depth.

The fault reactivation induces localized plastic shear strain distributed over a length of about 290 m with a maximum value of 4.5×10^{-3}, in a portion of the fault just below the reservoir (red zone in Fig. 6a). The full dynamic analysis showed that the rupture self-propagated as a result of fault-strength weakening such that the slip propagated outside the pressurized zone (Fig. 6a). The rupture occurred over about 0.4 s with a maximum co-seismic shear slip of about 4 cm (Fig. 6b) and a maximum slip velocity of about 0.6 m/s (Fig. 6c).

Based on the calculated co-seismic fault rupture length and mean shear slip displacement, the seismic moment magnitude M_w was estimated using relationships from seismology as described above. Assuming that the fault rupture takes place over a 1 km section along the strike of the fault (i.e. 1 km out-plane fault length from our two-dimensional (2D) model section), the moment

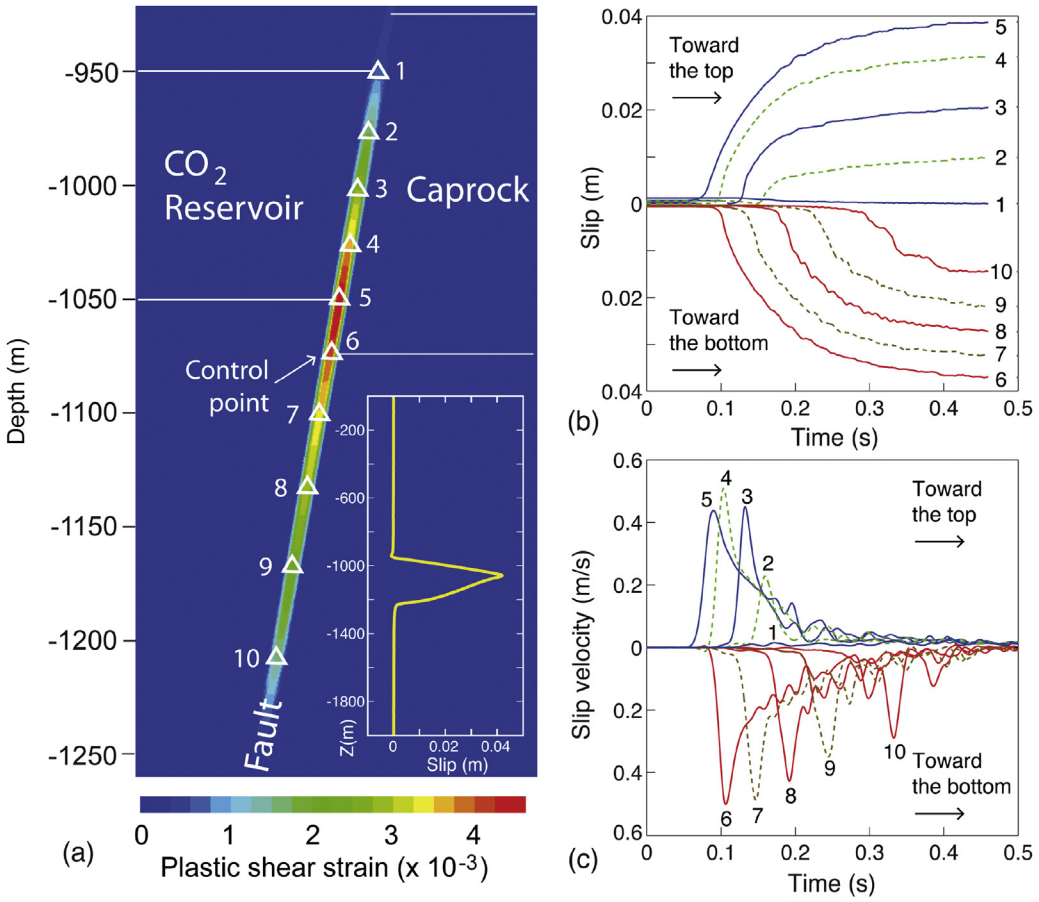

Fig. 6. Results from fully dynamic analysis of fault activation (Cappa and Rutqvist, 2012). (a) Plastic shear strain in the ruptured area and slip profile at the time of seismic rupture, and evolution of (b) slip and (c) slip velocity as function of time at different control points along the fault (white triangles on (a)). The rupture starts at the bottom of the CO_2 reservoir, near the control point 5.

magnitude M_w is estimated as 3. Alternatively, if assuming a circular rupture area with the diameter equal to the 290 m rupture length calculated from the plane strain analysis, the estimated moment magnitude M_w would be 2.5. We note that the magnitude in this case is a little lower than that for the previous analysis in Cappa and Rutqvist (2011b) summarized above in which the magnitude M_w was calculated as 3.4. The reason is the difference in depth, which in the previous analysis in Cappa and Rutqvist (2011b) was 1.5 km compared to 1 km in Cappa and Rutqvist (2012). At 1.5 km the absolute and differential stresses are higher, resulting in a higher reservoir pressure required for reactivation and a larger shear stress drop during reactivation.

The sudden fault rupture created a seismic source that generates waves and wave propagation that was calculated in FLAC3D dynamic calculation mode solving the full equations of motion in a fully nonlinear analysis (Cappa and Rutqvist, 2012). The generated seismic waves are attenuated by geometric spreading, pore fluid interaction, scattering, and a substantial dissipation which is associated with plastic flow in the fault and hits the ground surface resulting in a ground motion that was analyzed in Rutqvist et al. (2014), as to be described in the next subsection.

2.4. Effects on surface structures and human perception

Rutqvist et al. (2014) extended the dynamic fault activation study in Cappa and Rutqvist (2012), to analyze the simulated ground motions in terms of the potential for damage to ground surface structures and nuisance to the local human population. Ground vibrations were monitored at 15 stations along the ground surface in the model and the results were presented in terms of ground acceleration and velocity, and how these are distributed over multiple locations on the ground surface. In particular, the values of the peak ground acceleration (PGA) and peak ground velocity (PGV) were compared to U.S. Geological Survey's (USGS) instrumental intensity scales for earthquakes, and U.S. Bureau of Mines (USBM) vibration criteria associated with construction and mining activities, including blasting, as well as human perception vibration limits. Vibration criteria related to construction and mining activities, including blasting, were selected as a good analog to injection-induced seismic events, because of their similarities in terms of duration and frequency content (Bommer et al., 2006; Dowding and Meissner, 2011; Majer et al., 2012).

Fig. 7a and b shows the horizontal components of ground motions at a location where the fault intersects the ground surface and at another location a few hundred meters away from the fault. The blue, red and green lines represent different cases of a soft surficial soil layer. The simulation results in Rutqvist et al. (2014) showed locally strong PGA values up to 0.6 *g* close to the fault intersection with the ground surface, whereas PGA values away from the fault quickly attenuate to values below 0.1 *g*. A maximum PGV of about 40 mm/s also occurred close to the fault at the ground surface. We can also see the effects of the surficial soil layer which tends to damp some of the high frequency accelerations, meaning that the highest acceleration values in Fig. 7a are related to the case without a surficial soil layer and PGA = 0.6 *g* at 30–40 Hz. We can also observe in Fig. 7d a slightly higher PGV for a thicker soil layer (i.e.

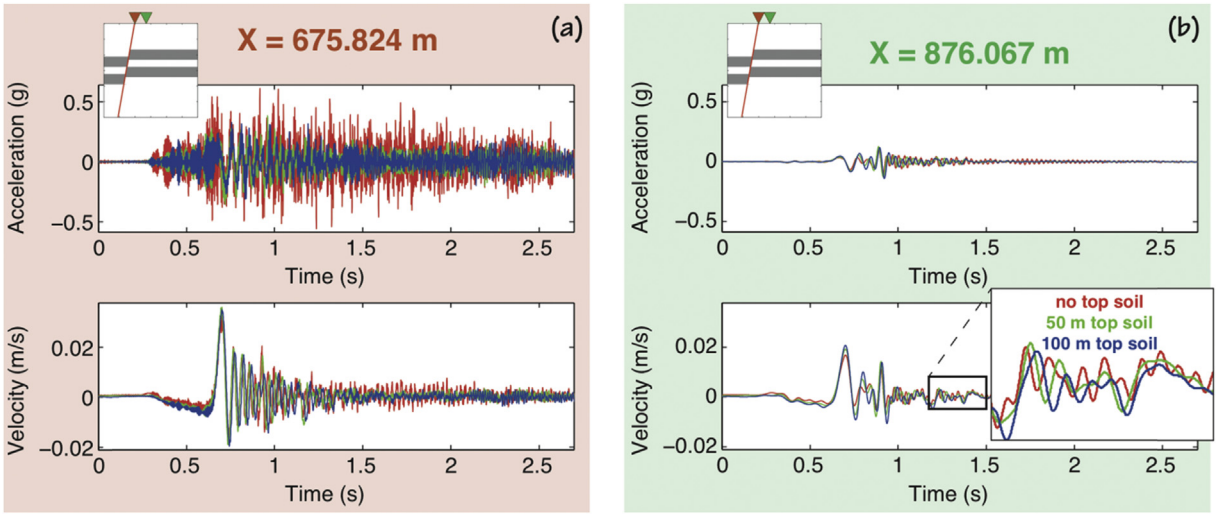

Fig. 7. Simulated horizontal acceleration and velocity components at (a) $X = 676$ m (on the top of fault) and (b) at $X = 876$ m (200 m from the fault) with and without a softer top soil layer (results from Rutqvist et al., 2014).

the soil layer amplified PGV), whereas without the soil layer, the PGV is about 30 mm/s and is associated with an initial pulse, one jolt, at a frequency of about 5–10 Hz.

Fig. 8 shows an overlay of the calculated ground motion at $X = 676$ m (at fault) in frequency spectrum on the USBM criterion (Siskind curve) and the human perception criterion. The "Z-curve or Siskind curve" shown as the blue line in Fig. 8 was originally published by Siskind et al. (1980) and shows the limits in peak particle velocity (PPV) in inch per second (ips), recommended by the USBM to preclude cosmetic damage to plaster and drywall. The red lines in Fig. 8 represents the human perception limits specified

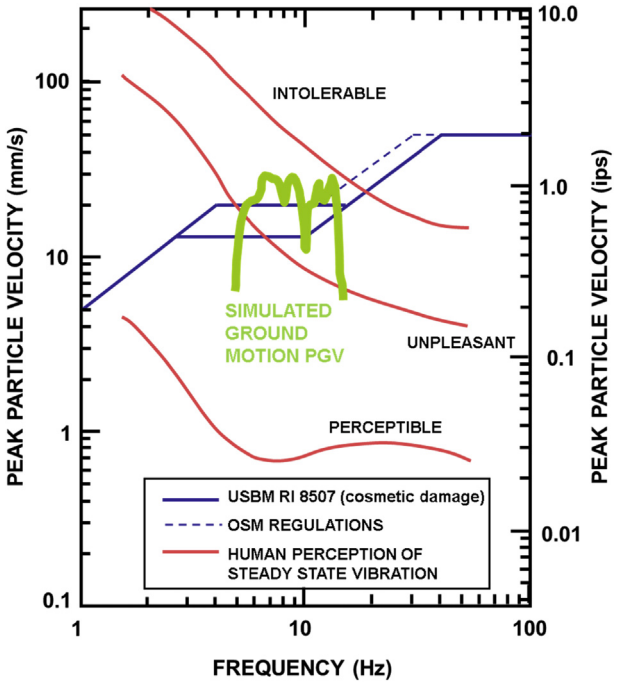

Fig. 8. Comparison of simulated PGV frequency spectrum (green line) for ground motion where the fault intersects the ground surface to the USBM criterion for cosmetic building damage and the human perception criterion (modified from Rutqvist et al., 2014).

in the U.S. Army Engineering Manual EM 1110-2-3800 (USACE, 1972). We see that the simulated PGV of around 25 mm/s over a frequency of 6–15 Hz (green line in Fig. 8) is just above the blue Siskind curve and could therefore potentially cause cosmetic damage (e.g. hairline fracture in drywall or plaster). Moreover, the simulated velocity is above the red line for unpleasant steady-state vibration, which implies that this short duration event would be clearly perceptible by humans.

If one would look at the maximum PGA of 0.6 *g*, and the USGS' empirically correlated instrumental intensity scale, a PGA of 0.6 *g* would correspond to an instrumental intensity of VIII, which would correspond to perceived severe shaking and moderate-to-heavy damage. However, as discussed in Rutqvist et al. (2014), USGS' criteria were developed based on tectonic events, which occur much deeper than shallow injection-induced seismic events. Thus, the results in Rutqvist et al. (2014) confirm the appropriateness of using PGV (rather than PGA) and frequency for the evaluation of potential ground-vibration effects on structures and humans from shallow injection-induced seismic events.

Finally, the study in Rutqvist et al. (2014) demonstrated for a synthetic case that the integrated analysis involving the chain of processes from cause to consequences could be done quantitatively. At a future injection site, such an analysis will require site-specific input parameters, including depth of injection zone, likely fault orientations and stress field, injection rates, and site-specific material properties. For a dynamic wave propagation and ground vibration analysis, it could also involve model calibration and testing of the velocity and attenuation properties against seismic data (if available). One of the key properties for fault reactivation modeling is the coefficient of friction of the fault and how it drops with shear. In Rutqvist et al. (2014), the coefficient of friction dropped from 0.6 to a residual value of 0.2 which may be considered as a conservative (worst case) scenario. A smaller difference between peak and residual shear strengths significantly reduces the seismic response such that seismicity would easily drop to levels that would result in ground vibrations not discernable by humans.

2.5. Links between seismicity and leakage

Rinaldi et al. (2014a) focused on the short-term integrity of the sealing caprock, and hence on the potential for leakage of either brine or CO_2 to reach the shallow groundwater aquifers during

active injection. Rinaldi et al. (2014a) calculated both seismic magnitude and potential leakage and thereby could investigate the link between seismicity and leakage. TOUGH-FLAC simulations were conducted considering reactivation of both minor (small offset) and major (large offset) faults and with consideration of a number of fault hydromechanical models for stress/strain-dependent permeability change during fault reactivation. The analysis in Rinaldi et al. (2014a) showed that whereas it is very difficult to predict how much fault permeability could change upon reactivation, this process can have a significant impact on the leakage rate. Moreover, the analysis showed that induced seismicity associated with fault reactivation may not necessarily open up a new flow path for upward CO_2 leakage. In fact, much of the reactivation tended to take place below the reservoir, rather than above it. Fig. 9 shows one example in which a $M_w = 2.7$ event resulted in co-seismic slip below the reservoir, whereas the total slip and permeability changes are affected by longer-term aseismic shear, which creates a flow path upward from the reservoir. However, the upward CO_2 migration was then diverted into another permeable layer and as a result no upward leakage toward the ground surface occurred. Results therefore showed a poor correlation between earthquake magnitude and amount of fluid leakage, highlighting that a single event is generally not enough to substantially change the permeability along the entire fault length. Consequently, even if some changes in permeability occur, this does not mean that CO_2 will migrate upward along the entire fault, breaking through the caprock to enter an overlying aquifer. This is in agreement with studies of Nordbotten et al. (2009) who showed that even in the case of leakage through the primary caprock (the one directly overlying the CO_2 storage unit), unless the leakage pathway leads continuously and directly to protected groundwater or to the land surface, the leaked CO_2 will be trapped in overlying strata in secondary traps (reservoirs or deep saline aquifers) due to the layered nature of the sedimentary structure (Celia et al., 2015).

The above studies have been done for a subvertical fault in which injection reservoir was located in the hanging-wall of the fault. However, as shown in TOUGH-FLAC modeling by Konstantinovskaya et al. (2014), the localization of shear failure along high-angle normal faults is very much dependent on the location of the injection zone relative to the inclined fault plane. In Konstantinovskaya et al. (2014), modeling was performed to simulate CO_2 injection into a storage reservoir bounded by two subvertical faults in the St. Lawrence Lowlands sedimentary basin, Quebec, Canada. The modeling showed that when the injection reservoir was in the footwall of the fault plane, the shear failure was initiated along the fault segment located above the targeted reservoir. In contrast, when the injection took place in the hanging-wall reservoir, the rupture occurred along a fault segment located at the reservoir level and below it. Thus, there might be a higher potential of upward CO_2 leakage if a fault is reactivated by reservoir pressurization on the footwall of the fault. Such a difference between hanging and footwall fault activation makes the link between seismicity and leakage even more uncertain.

2.6. Effects of heterogeneous fault properties

In the above studies, it was assumed that fault properties were homogenous along the fault planes, though in reality fault properties can be strongly heterogeneous, affected by the variation in host rock properties adjacent to the fault. To study the effect of heterogeneous fault properties, Jeanne et al. (2014) performed in situ multidisciplinary analyses of two different fault zones in carbonate formations, one major (several kilometers long) seismically active fault and another small fault zone (a few hundred meters long). The fault zones characterized in detail in the field were represented in the coupled TOUGH-FLAC modeling with markedly different fault architectures, in which the fault damage zone in the smaller immature fault zone was discontinuous with very heterogeneous mechanical and hydraulic properties (Fig. 10a and b). The modeling showed that such heterogeneity favors rapid damage zone pressurization, resulting in small earthquakes and also limits the potential CO_2 leakage at rupture. For example, Fig. 10a and b displays a marked difference in fluid pressure distribution after 1 year of injection in which pressure diffusion is prevented in the case of an immature fault (Fig. 10a).

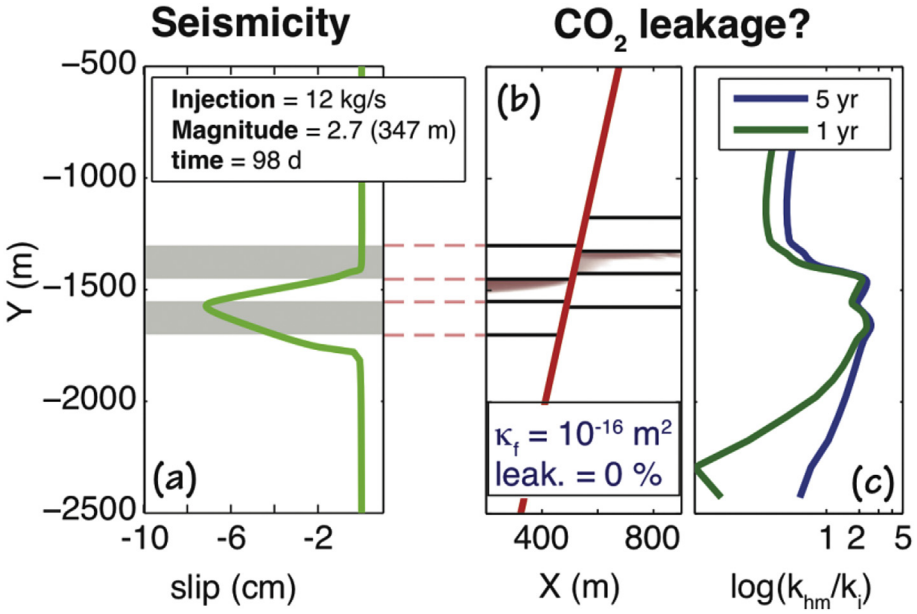

Fig. 9. Example of fault activation modeling in Rinaldi et al. (2014a) showing for a case of reactivation of an offset reservoir bounding fault when a $M_w = 2.7$ seismic event (a) does not result in any upward CO_2 leakage as the CO_2 is diverted into another overlying permeable layer (b) despite fault permeability change by 2 orders of magnitude (c).

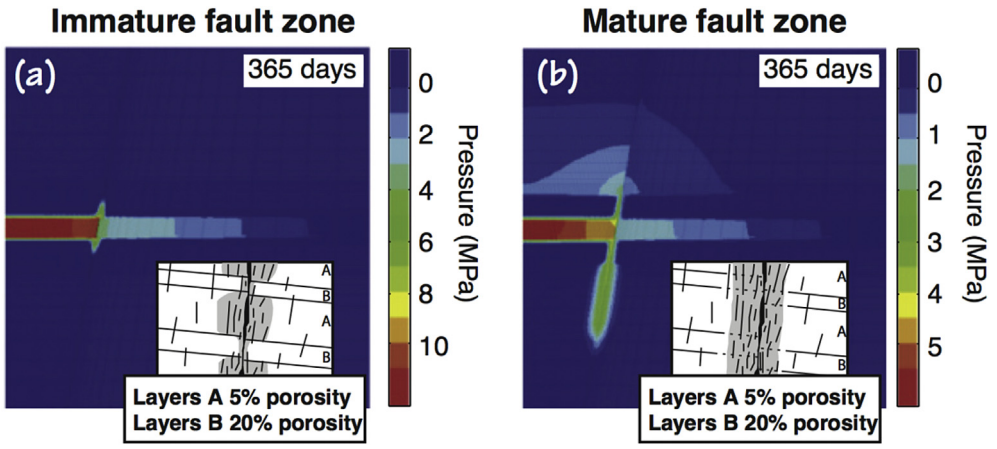

Fig. 10. Results from Jeanne et al. (2014) showing the difference in fluid pressure migration in the case of reactivation of (a) a smaller immature fault with heterogeneous fault permeability and (b) a major mature fault with continuous permeability along the fault. Inserts show conceptual models of the two types of faults.

Rinaldi et al. (2014b) also studied the influence of fault zone architecture on pore pressure distribution and on the resulting fault reactivation, but for a case of a shale-sandstone sequence of multiple caprock and reservoir layers. Results showed how the presence of hydraulic and mechanical heterogeneities along the fault influences the pressure distribution along the fault itself, as well as the evolution of effective normal and shear stresses. One example of simulation results from Rinaldi et al. (2014b) is shown in Fig. 11. Fig. 11 shows that for homogenous fault properties, the co-seismic rupture and seismic magnitude are larger and the pressure can migrate over much longer distance along the fault damage zone. Overall the results in Rinaldi et al. (2014b) showed that hydromechanical heterogeneities (1) strengthen the fault zone resulting in smaller earthquakes, and (2) impede upward fluid migration along the fault. Moreover, studies on the effects of the caprock (Fig. 11) and aquifer thickness showed that a thin caprock or aquifer leads to smaller events, but a much higher percentage of leakage through the caprock and into the upper aquifer, whereas the amount of leakage is drastically reduced in the case of a multi-caprock, multi-aquifer system.

2.7. 3D vs. 2D modeling and effects of well orientation

All the above simulations were conducted in 2D plane strain models. As a result, some uncertainties in the evaluation of the moment magnitude exist due to necessary assumptions on rupture area estimates in the 3rd dimension. Full three-dimensional (3D)

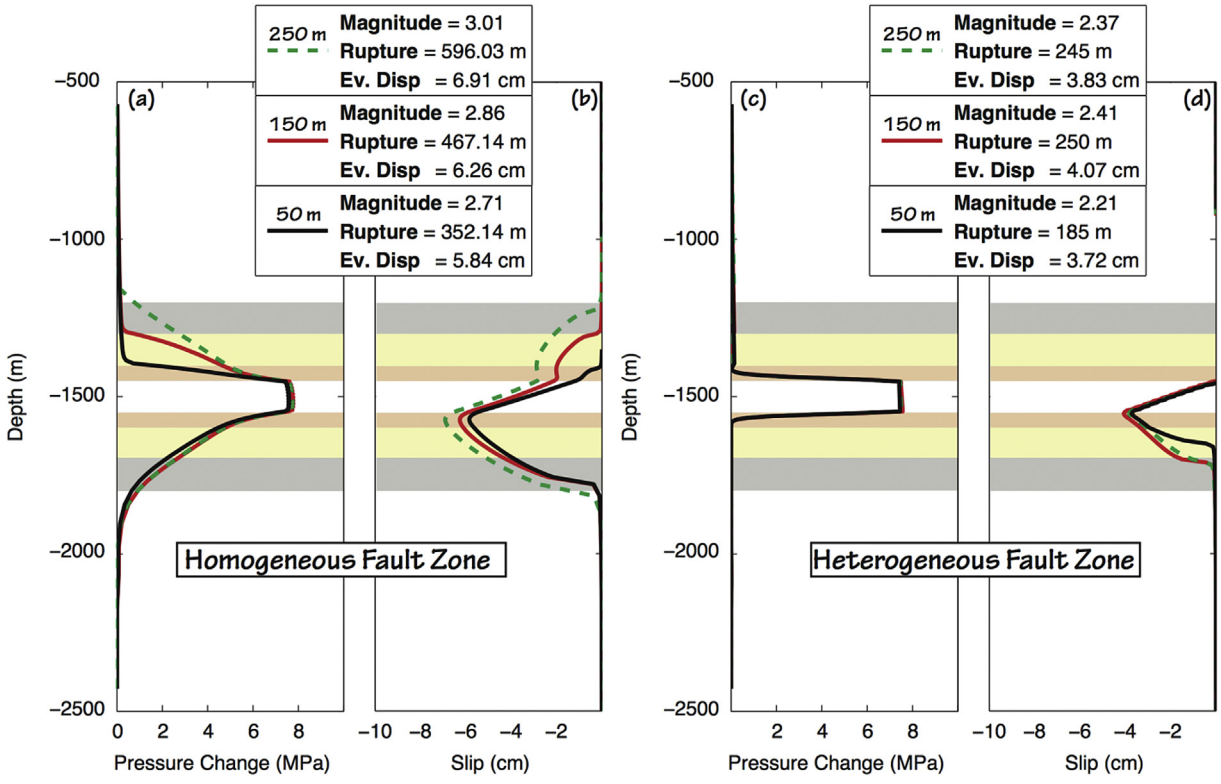

Fig. 11. Results from Rinaldi et al. (2014b) showing the effects of caprock thickness for homogeneous (a, b) and heterogeneous (c, d) fault properties.

TOUGH-FLAC analyses were conducted in Rinaldi et al. (2015) to investigate the effects of well geometry (vertical vs. horizontal injection well) on seismic fault rupture and CO_2 leakage. Simulation results for the vertical well showed faster and more localized fault pressurizing than that for the horizontal well, resulting in a smaller seismic event. For a horizontal well, the pressure is distributed over a wider area along the fault, which requires a longer time for reactivation, but results in a larger event. In these 3D simulations, changes in permeabilities of damage zone and fault-core were considered. Although the calculated fault permeability enhancement is similar for the two cases, results showed a slightly higher leakage rate for the vertical well in the region close to the well itself, while the leakage resulting from injection through the horizontal well is more widely distributed. Overall, the simulations showed that the seismic magnitudes calculated in the full 3D simulations were within the range of those calculated in the 2D analysis, bounded by the values of the 2D analysis for the assumption of circular rupture area and 1 km rupture along the fault strike. In general, the assumption of circular rupture areas somewhat underestimates the seismic magnitude as the rupture tends to be more elongated along the strike of the fault (Fig. 12).

2.8. Depth-dependent fault rheology through rate-dependent friction

Finally, the current development of TOUGH-FLAC related to fault activation includes the implementation and application of a slip-rate dependent fault friction. Urpi et al. (2016) presented the first step in which slip- and rate-dependent fault friction, in the framework of the rate-and-state "slowness law", and inertial effects were taken into account during rupture. Contact elements were used to take into account the frictional behavior of the rupture plane. Different scenarios of fault rheologies at different depths were defined based on published laboratory data on CO_2-saturated intact and crushed rock samples, representative of a potential target aquifer, sealing formation and fault gouge (Verberne et al., 2014; Pluymakers and Niemeijer, 2015). Assuming fault-healing after rupture, repeated seismic events can be simulated due to fluid pressurization. The total cumulative slip, in principle, can be larger than the size of the contact element, because the contact points of the various interfaces can be updated. The simulations in Urpi et al. (2016) show that the first triggered rupture always produces the largest rupture length and slip magnitude, both of which correlate with the fault rheology. Velocity weakening produces larger ruptures and generates larger magnitude seismic events. Fig. 13 shows the model and an example of simulation results displaying the effect of velocity weakening friction. In all the cases, the fault portion within the caprock and overburden was assumed velocity neutral, but fault rupture could extend into this zone in the case of strong velocity weakening in the reservoir and underburden. On the other hand, nucleation of rupture in a velocity strengthening fault section always resulted in a limited rupture in terms of maximum slip and rupture length, and ground acceleration less than 0.015 *g*, which would be too small to be felt by humans. Again, this shows the importance of characterizing fault properties, because a more brittle (velocity weakening) behavior is necessary for producing seismic events that could be felt and potentially create a leakage path through the caprock.

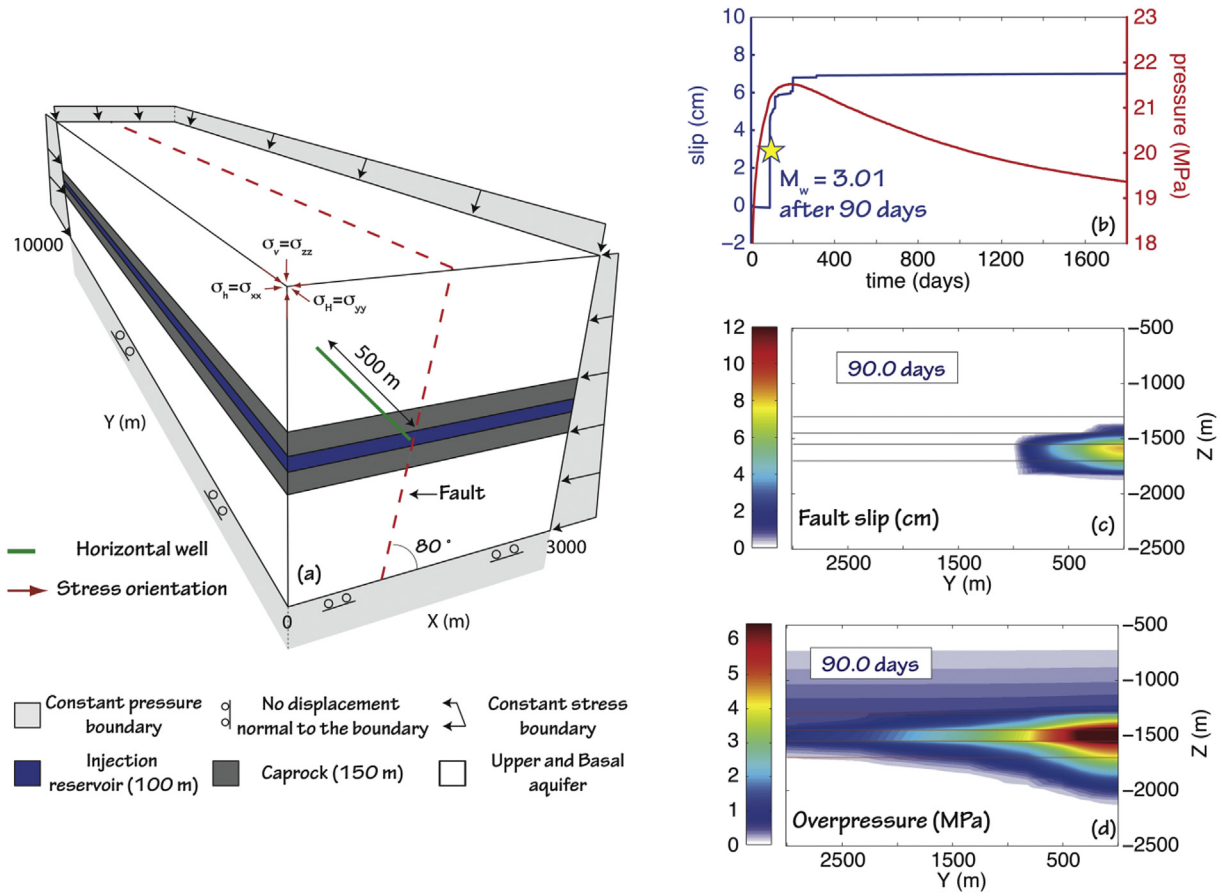

Fig. 12. 3D model and simulation results from Rinaldi et al. (2015) showing pressure and slip evolution, co-seismic rupture area and pressure distribution on the fault plane.

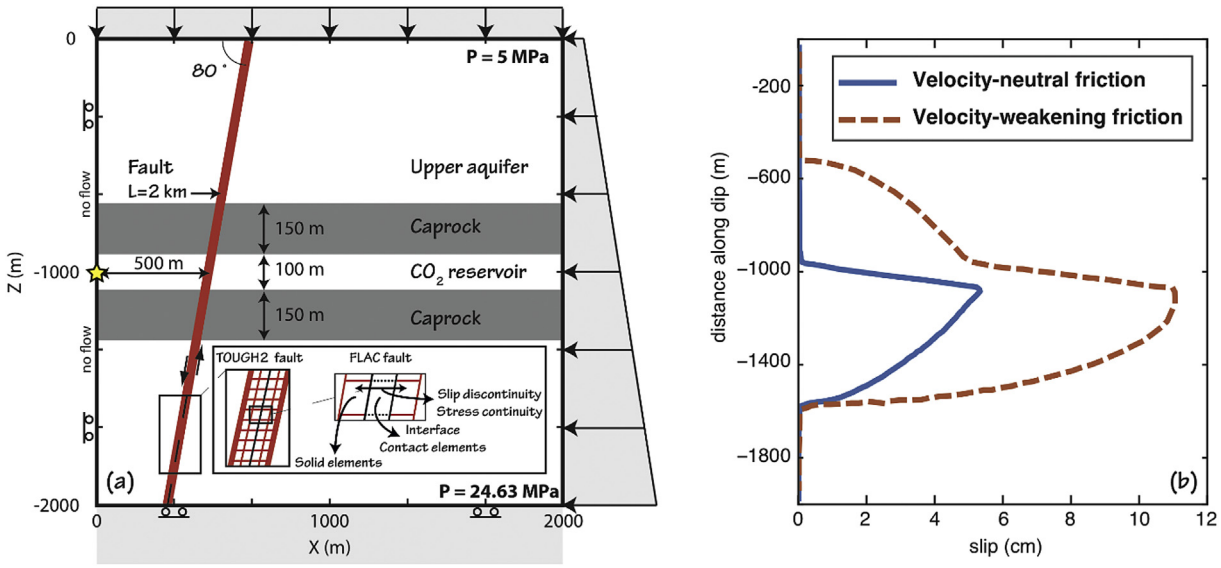

Fig. 13. Model and simulation results from Urpi et al. (2016) showing how the rupture could propagate up through the caprock in the case of stronger velocity weakening fault frictional properties.

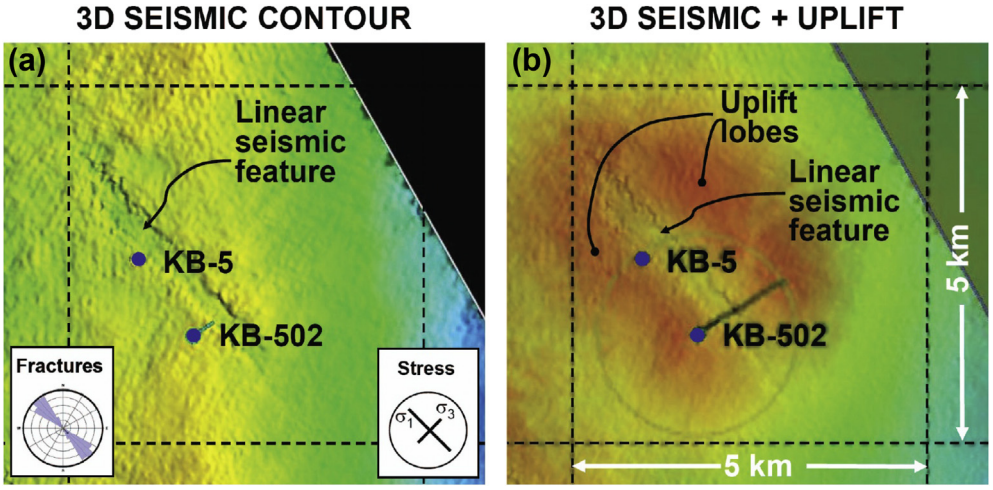

Fig. 14. Results from 3D seismic survey in northern Krechba in 2009, showing a deep linear feature and its correlation with surface uplift, natural fractures, and stress orientation (Rutqvist, 2012): (a) 3D seismic contour extracted from Gibson-Poole and Raikes (2010) and Wright (2011) showing contour layer at the top of the C20.1 unit, about 150 m above the injection zone (at a depth of about 1.7 km), and (b) 3D seismic contour results overlain by ground surface uplift evaluated from InSAR data of MDA and Pinnacle Technology (Wright, 2011). In (a) red and yellow correspond to high elevation, whereas blue corresponds to low elevation, indicating a push down in the seismic signature along the linear feature. In (b), red contour represents the maximum uplift, in the order of 2 cm.

3. Lessons learned from In Salah modeling

The In Salah CO_2 storage project (Mathieson et al., 2011; Ringrose et al., 2013) provides a good example for studies of potential fault reactivation during CO_2 injection. The injection pressure was quite substantial (up to about 10 MPa downhole overpressure from an initial reservoir pressure of about 17.5 MPa) and the injection zone (a 20 m thick sandstone layer at about 1900 m depth) is intersected by many subvertical minor faults observed from 3D seismic surveys (Iding and Ringrose, 2010; Ringrose et al., 2011). Moreover, InSAR data on ground surface deformation had such a good spatio-temporal resolution that it would be possible to detect potential injection-induced fault responses (Vasco et al., 2010; Bissell et al., 2011; Mathieson et al., 2011). In particular, at one of the three horizontal injection wells, injection well KB-502, a complex surface deformation pattern was observed, including two parallel uplift lobes rather than one single uplift lobe (Fig. 14). This double-lobe uplift pattern was first interpreted by Vasco et al. (2010) to signify the opening of a linear feature within and around the injection zone, i.e. at around 1900 m depth. Similarly, using multiphase fluid flow and geomechanical numerical modeling, Rutqvist et al. (2011) as well as Morris et al. (2011) also concluded that the opening of a vertical feature could explain the observed double-lobe uplift. The first TOUGH-FLAC analysis of such double-lobe uplift is shown in Fig. 15, indicating a qualitative agreement with the double-lobe uplift pattern shown in Fig. 14. This was achieved using anisotropic elastic properties within the fault zone, which was considered to be a highly fractured medium.

At the same time, the analysis of a 3D seismic survey indicated that such a fractured zone may indeed intersect the injection well KB-502, with a linear feature visible in the seismic signature up to a

few hundred meters above the injection zone (Gibson-Poole and Raikes, 2010; Wright, 2011; Ringrose et al., 2013). As shown in Fig. 14, the linear feature aligns precisely parallel with the dominant fracturing orientation, exactly perpendicular to the minimum compressive principal stress, and it is well correlated with the double-lobe uplift on the ground surface (Rutqvist, 2012). This very precise linear alignment may indicate the opening of fractures (which exist in the lower part of the caprock) or a fractured rock zone, or creation of new fractures, rather than opening or reactivation of a fault.

Rinaldi and Rutqvist (2013) applied TOUGH-FLAC to conduct a detailed coupled multiphase fluid flow and geomechanical analysis of the fracture zone responses with simultaneous matching of injection pressure and uplift (both in time and space). In the model simulations, the fracture zone was simulated using an orthotropic model, characterized by a strong anisotropy: the porous medium can deform more in the direction normal to the plane than that along the plane. The fracture zone properties were determined by model calibration to achieve a good match with field data for a fracture zone 3500 m long and extending 350 m above the reservoir (Fig. 16). The InSAR and injection data were interpreted such that the fracture zone activates and becomes permeable in response to increasing reservoir pressure after only a few months of CO_2 injection (Fig. 17c). Using such a model, the displacement on the satellite's line of sight features a double-lobe uplift and a magnitude close to the measured InSAR data (Fig. 17).

A sensitivity study showed that changes in the fracture zone height from reservoir depth produce results that in some cases significantly deviate from field observations. Specifically, when the fracture zone is assumed to penetrate into the upper aquifer, a double-lobe pattern was still achieved, but the calculated uplift time evolution showed a trend completely different from field observation. The poor fit occurred when assuming a substantial pressure release up into the shallow aquifer. Consequently, the analysis by Rinaldi and Rutqvist (2013) supports the notion that the fracture zone is confined within the caprock and does not penetrate the overlying aquifer.

Another relevant observation from In Salah is that a number of minor subvertical faults crossing the reservoir have been mapped from the 3D seismic surveys (Ringrose et al., 2011). However, CO_2 injection at In Salah has not resulted in any felt seismic events or substantial strike-slip shear movements in the prevailing strike-slip stress field. If strike-slip shear movement had occurred, it would have surely been observed as asymmetric uplift pattern on each side of such a fault. On the other hand, several thousands of micro-seismic events have been detected with the maximum reported magnitude M_w of 1.7 (Stork et al., 2015). Most of these events were localized to be close to KB-502 well in NW–SE orientation, which is along the direction of maximum principal stress and along the direction of the dominant fracture direction, coinciding with fracture zone orientation. Analysis of the same seismic data by Goertz-Allmann et al. (2014) came to the same conclusion and argued from the seismic data that it is feasible that new fractures were created at high wellhead pressures. They concluded that reservoir fracture pressure of the injection horizon has most likely been exceeded occasionally, accompanied by increased micro-seismic activity. This occurred at a threshold wellhead pressure of about 15.5 MPa, which according to Rinaldi and Rutqvist (2013) calculations would correspond to a downhole reservoir overpressure of about 10 MPa. The caprock at In Salah is 950 m thick, comprising a number of thick, resilient seals. Even though fracturing may have penetrated the lower caprock units, the overall integrity of the storage site is maintained. These findings by the TOUGH-FLAC modeling of In Salah have been corroborated by White et al. (2014) and Verdon et al. (2015).

Finally, the In Salah project is an example at which induced micro-seismicity occurred in the sedimentary sequence, but at a substantial downhole injection pressure close to the fracturing pressure. The deep fault response was discovered through monitoring of surface deformations. But if the micro-seismic network had been installed already from the beginning of the injection, the clear pressure threshold could have been determined. As a result, the injection pressure could have been managed to prevent further fracturing and induced seismicity.

4. Concluding remarks and recommendations

Although no felt seismic event has been reported from any of the current or past CO_2 storage projects, it should be recognized that potential future commercial GCS operations from large power plants will require injection at a much larger scale. Experience from injection activities in related industries (e.g. waste-water injection, hydrocarbon exploitation, enhanced geothermal systems developments, and reservoir impoundments) shows that induced seismicity issues should be carefully considered in developing new GCS projects (Gupta, 1992; Cypser and Davis, 1998; Segall and Fitzgerald, 1998; Häring et al., 2008; Majer et al., 2012; The National Research Council, 2012; Weingarten et al., 2015). In future large scale GCS, large-scale pressure buildup, associated crustal straining, and the potential presence of undetected faults may be of greatest concern (Rutqvist, 2012). The risk is generally expected to increase with injection volume, since this will increase

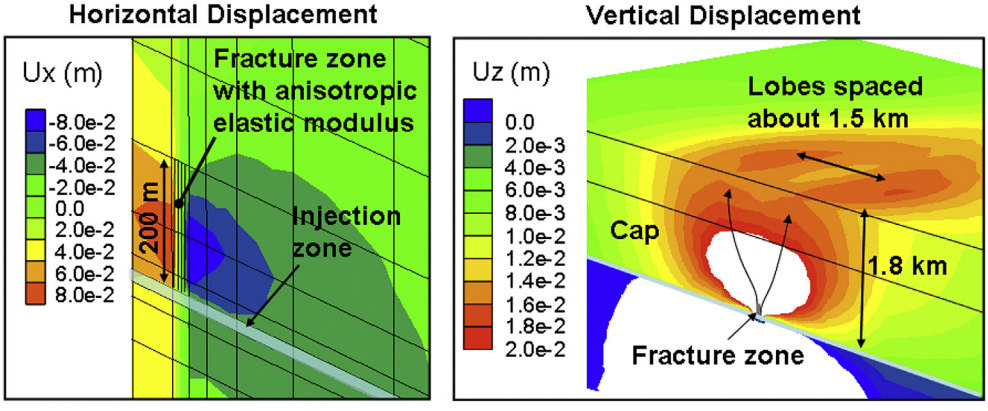

Fig. 15. TOUGH-FLAC forward coupled numerical modeling of CO_2 injection, with pressure inflation of the vertical fracture zone, which results in a double-lobe uplift response on the ground surface similar to observations shown in Fig. 14 (Rutqvist et al., 2010).

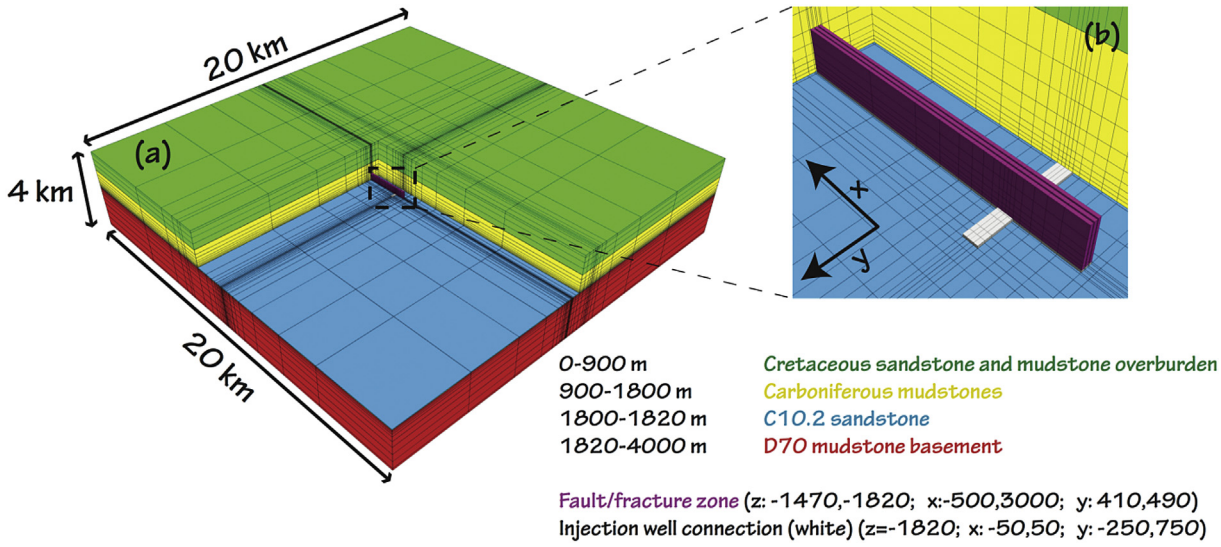

Fig. 16. (a) Mesh grid used in the coupled TOUGH-FLAC model (about 30,000 gridblocks); and (b) enlargement of the injection area and fracture zone (Rinaldi and Rutqvist, 2013).

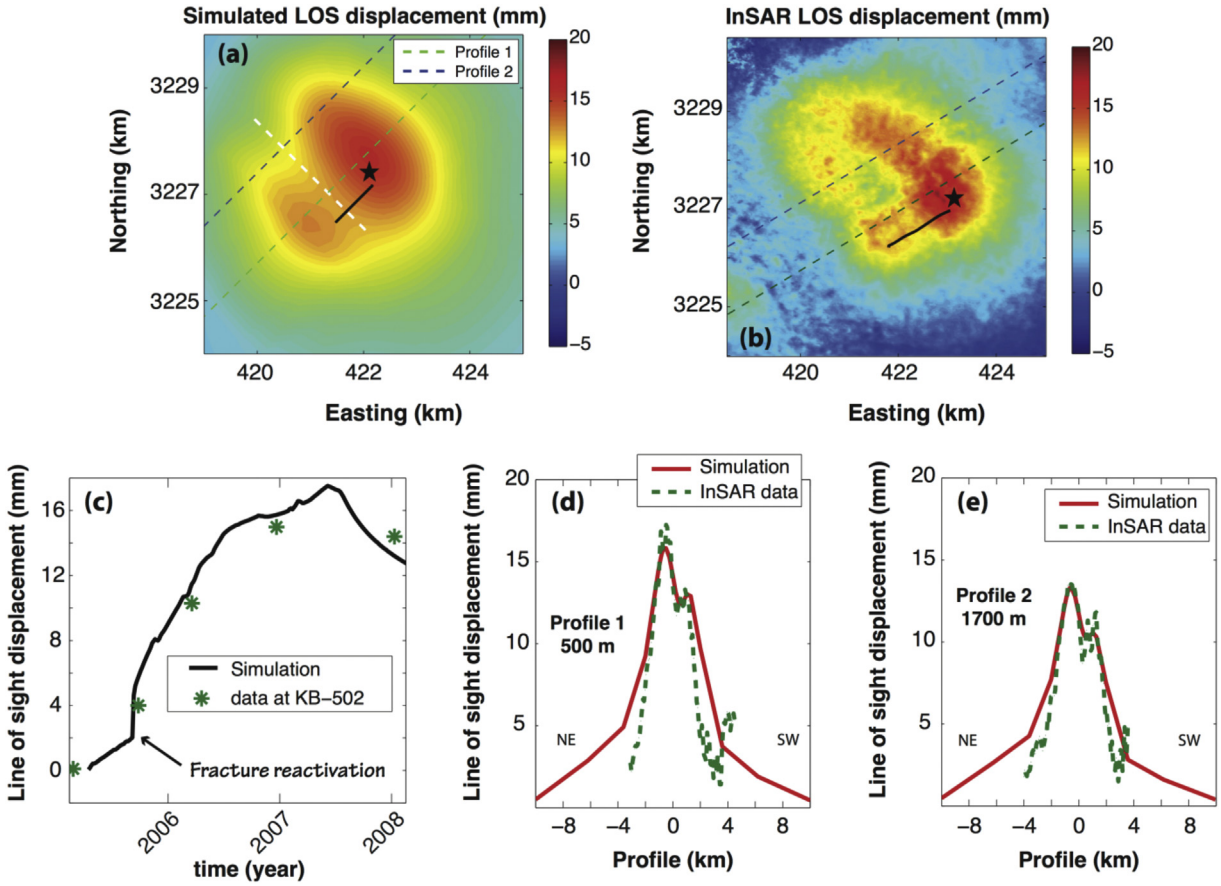

Fig. 17. Comparison between TOUGH-FLAC simulated displacement and InSAR data (Rinaldi and Rutqvist, 2013). (a) Resulting displacement in the satellite line of sight. Black segment represents the KB-502 injection well. White, dashed segment represents the simulated fracture zone direction. Green and blue, dashed lines represent the direction of two profiles for the comparison with InSAR data at 500 m and 1700 m from the injection well, respectively. (b) InSAR data after 618 days of injection (23 December 2006). (c) Comparison between simulated and observed ground surface uplifts. (d) Comparison between simulation (red line) and InSAR data (green, dashed line) along the profile 1 (500 m from the injection well). (e) Comparison between simulation (red line) and InSAR data (green, dashed line) along the profile 2 (1700 m from the injection well).

the probability that the expanding reservoir pressurization reaches near critically stressed faults of larger dimensions. To deal with this issue, a best-practice framework is needed for the site-investigations phase of a GCS project. This should comprehend site-geological-screening for the appreciation of major fault characteristics and behavior, structural investigation for the understanding of past stress fields, and geophysical surveys for the creation of a conceptual model of the reservoir system. The

framework should also involve literature review of the historical natural seismicity, assessment of the potential for induced seismicity as part of the created conceptual model, and recommended steps for mitigation of the risk of the induced seismicity, as well as addressing the human element (Myer and Daley, 2011).

The TOUGH-FLAC deterministic fault activation modeling summarized in this paper demonstrates that a fault rupture in the order of 1 km will be required to create an injection-induced event (e.g. in the magnitude of 4) that could be widely felt on the ground surface. The resulting seismic magnitude and potential for creating a leakage path through overburden sealing layers (caprock) depends on the number of parameters such as fault orientation, stress field, injection location relative to the fault, and rock properties. Model simulations further demonstrate that seismic events large enough to be felt by humans require brittle fault properties and continuous fault permeability allowing for the pressure to be distributed over a large fault patch that ruptures at once. Heterogeneous fault properties, which are commonly encountered in faults intersecting multilayered shale/sandstone sequences, effectively reduce the likelihood of inducing felt seismicity and also effectively impede upward CO_2 leakage. A number of simulations show that even a sizable seismic event that could be felt may not be capable of opening new flow paths across the entire thickness of an overlying caprock. Additionally, such flow paths are very unlikely to cross a system of multiple overlying caprock units.

The modeling of the In Salah CO_2 storage site showed possible fracturing of the caprock and opening of deep fracture zone that was also associated with induced micro-seismicity. Induced microseismicity could occur because the reservoir consisted of relatively tight, but fractured and brittle sandstone. However, this occurred at substantial reservoir pressure of about 160% the hydrostatic pressure, which is close to the magnitude of the least principal stress.

The type of coupled fluid flow and geomechanical fault activation modeling used in most of the simulations quoted in this paper can be used to guide the injection design at future CO_2 injection sites. In fact, early in the site screening, simplified models may be preferable for first-order analysis and quick assessment of CO_2 injection-site suitability. The simplified models may be analytical and semi-analytical models (e.g. Streit and Hillis, 2004; Mathias et al., 2009), or models based on simplified equations for efficient solutions (Nordbotten and Celia, 2006; Celia et al., 2015), or numerical multiphase flow models linked with analytical geomechanical models (e.g. Lucier et al., 2006; Chiaramonte et al., 2008). Nevertheless, making an absolutely exact prediction of seismicity and an estimation of the maximum earthquake magnitude is very difficult. Continuous monitoring of geomechanical changes (such as ground surface deformations and induced microseismicity) is vital for tracking underground fluid pressure evolution, possibly detecting emerging fault reactivations, and providing an early detection of potential CO_2 migration out of the storage formation. This would ideally involve a staged approach with an initially longer-term injection, accompanied by seismic and surface deformation monitoring to determine how prone the site is to inducing seismicity. Such experiment and monitoring can also provide the necessary data on site-specific seismicity (if any) to make predictions for long-term operational conditions and might help to estimate how high the injection pressure can be without causing seismicity.

As discussed in this paper, a very important factor for induced seismicity and leakage is whether the rocks are brittle or ductile. It is well known from accumulation of hydro-carbon resources over geological time that the mechanical properties of the top seal units are critical in determining how shear reactivation could change the sealing capacity of a caprock unit (Ingram and Urai, 1999). The shear strength of mudstone and shale could be very low, with friction angle as low as 10°. However, despite low strength, a caprock unit consisting of soft plastic (ductile) rock can deform in a plastic but self-sealing way, and might therefore be more favorable than a stiff, brittle and dilatant rock. A relevant example might be the Gulf (of Mexico) Coastal area, characterized as a passive continental margin where recently active listric normal faulting resulting from sediment loading defines the regional stress regime (Zoback and Zoback, 1989). The least horizontal compressive principal stress in the Gulf Coast area has been estimated to be about 60% of the lithostatic (vertical) stress (Zoback and Zoback, 1989), i.e. a horizontal-to-vertical stress ratio of 0.6. However, although faults may be on the verge of shear instability and could be activated by injection, the sediments are very soft, including unconsolidated reservoir sands and shale layers that are self-sealing. Thus, even if such faults are activated, this activation will most likely not cause any seismicity or substantial leakage.

Thus, we emphasize the importance of site investigation to characterize rock properties and if at all possible to avoid brittle rock such as crystalline basement or sites in hard and brittle sedimentary sequences that are prone to induced seismicity and permanent damage. Efforts should be made to identify sites in more ductile rock formations that can accommodate aseismically stress and strain induced by the injection. Ideally the injection should take place in a reservoir below multiple ductile caprocks that can self-heal and still provide protection of shallow groundwater resources that should fault activation occur at depth.

Conflict of interest

The authors wish to confirm that there are no known conflicts of interest associated with this publication and there has been no significant financial support for this work that could have influenced its outcome.

Acknowledgments

This work was funded by the Assistant Secretary for Fossil Energy, National Energy Technology Laboratory, National Risk Assessment Partnership of the U.S. Department of Energy under Contract No. DEAC02-05CH11231. A. P. Rinaldi is currently funded by a Swiss National Science Foundation (SNSF) Ambizione Energy grant (PZENP2_160555).

References

Bissell RC, Vasco DW, Atbi M, Hamdani M, Okwelegbe M, Goldwater MH. A full field simulation of the In Salah gas production and CO_2 storage project using a coupled geo-mechanical and thermal fluid flow simulator. Energy Procedia 2011;4:3290–7.

Bommer JJ, Oates S, Cepeda JM, Lindholm C, Bird J, Torres R, Marroquín G, Rivas J. Control of hazard due to seismicity induced by a hot fractured rock geothermal project. Engineering Geology 2006;83(4):287–306.

Cappa F, Rutqvist J. Modeling of coupled deformation and permeability evolution during fault reactivation induced by deep underground injection of CO_2. International Journal of Greenhouse Gas Control 2011a;5(2):336–46.

Cappa F, Rutqvist J. Impact of CO_2 geological sequestration on the nucleation of earthquakes. Geophysical Research Letters 2011b;38(17). http://dx.doi.org/10.1029/2011GL048487.

Cappa F, Rutqvist J. Seismic rupture and ground accelerations induced by CO_2 injection in the shallow crust. Geophysical Journal International 2012;190(3):1784–9.

Cappa F, Rutqvist J, Yamamoto K. Modeling crustal deformation and rupture processes related to upwelling of deep CO_2 rich fluids during the 1965–1967 Matsushiro earthquake swarm in Japan. Journal of Geophysical Research: Solid Earth 2009;114:B10304. http://dx.doi.org/10.1029/2009JB006398.

Celia MA, Bachu S, Nordbotten JM, Bandilla KW. Status of CO_2 storage in deep saline aquifers with emphasis on modeling approaches and practical simulations. Water Resources Research 2015;51(9):6846–92.

Chiaramonte L, Zoback MD, Friedmann J, Stamp V. Seal integrity and feasibility of CO_2 sequestration in the Teapot Dome EOR pilot: geomechanical site characterization. Environmental Geology 2008;54(8):1667–75.

Cypser AC, Davis SD. Induced seismicity and the potential for liability under U.S. law. Tectonophysics 1998;289(1–3):239–55.

Dowding CH, Meissner JE. Interpretation of microseismic effects of petroleum production through observed response to coal mine blasts. In: Proceedings of the 45th U.S. Rock Mechanics/Geomechanics Symposium, vol. 1. New York: Curran Associates, Inc.; 2011. p. 1–8.

Ellsworth WL. Injection-induced earthquakes. Science 2013;341(6142):1225942. http://dx.doi.org/10.1126/science.1225942.

Gibson-Poole CM, Raikes S. Enhanced understanding of CO_2 storage at Krechba from 3D seismic. In: Proceedings of the 9th Annual Conference on Carbon Capture and Sequestration. Pittsburgh, Pennsylvania; 2010.

Goertz-Allmann BP, Kuhn D, Oye V, Bohloli B, Aker E. Combining microseismic and geomechanical observations to interpret storage integrity at the In Salah CCS site. Geophysical Journal International 2014;198(1):447–61.

Gupta HK. Reservoir induced earthquakes. New York: Elsevier; 1992.

Hanks TC, Kanamori H. A moment magnitude scale. Journal of Geophysical Research: Solid Earth 1979;84(B5):2348–50.

Häring MO, Schanz U, Ladner F, Dyer BC. Characterisation of the Basel 1 enhanced geothermal system. Geothermics 2008;37(5):469–95.

Hornbach MJ, DeShon HR, Ellsworth WL, Stump BW, Hayward C, Frohlich C, Oldham HR, Olson JE, Magnani MB, Brokaw C, Luetgert JH. Causal factors for seismicity near Azle, Texas. Nature Communications 2015;6:6728.

Horton S. Injection into subsurface aquifers triggers earthquake swarm in central Arkansas with potential for damaging earthquake. Seismological Research Letters 2012;83(2):250–60.

Iding M, Ringrose P. Evaluating the impact of fractures on the performance of the In Salah CO_2 storage site. International Journal of Greenhouse Gas Control 2010;4(2):242–8.

Ingram GM, Urai JL. Top-seal leakage through faults and fractures: the role of mudrock properties, vol. 158. London: Geological Society; 1999. p. 125–35. Special Publication.

Itasca Consulting Group. FLAC3D V5.0, fast Lagrangian analysis of continua in 3 dimensions, user's guide. Minneapolis, USA: Itasca Consulting Group; 2011.

Jeanne P, Guglielmi Y, Cappa F, Rinaldi AP, Rutqvist J. The effects of lateral property variations on fault-zone reactivation by fluid pressurization: application to CO_2 pressurization effects within major and undetected fault zones. Journal of Structural Geology 2014;62:97–108.

Juanes R, Hager BH, Herzog HJ. No geologic evidence that seismicity causes fault leakage that would render large-scale carbon capture and storage unsuccessful. Proceedings of the National Academy of Sciences of the United States of America 2012;109(52):E3623. http://dx.doi.org/10.1073/pnas.1215026109.

Kanamori H, Anderson DL. Theoretical basis of some empirical relations in seismology. Bulletin of the Seismological Society of America 1975;65:1073–95.

Keranen K, Weingarten M, Abers GA, Bekins BA, Ge S. Sharp increase in central Oklahoma seismicity since 2008 induced by massive wastewater injection. Science 2014;345:448–51.

Konstantinovskaya E, Rutqvist J, Malo M. CO_2 storage and potential fault instability in the St. Lawrence Lowlands sedimentary basin (Quebec, Canada): insights from coupled reservoir-geomechanical modeling. International Journal of Greenhouse Gas Control 2014;22:88–110.

Lucier A, Zoback M, Gupta N, Ramakrishnan TS. Geomechanical aspects of CO_2 sequestration in a deep saline reservoir in the Ohio River Valley region. Environmental Geosciences 2006;13(2):85–103.

Majer E, Nelson J, Robertson-Tait A, Savy J, Wong I. Protocol for addressing induced seismicity associated with enhanced geothermal systems. U.S. Department of Energy; 2012.

Mathias SA, Hardisty PE, Trudell MR, Zimmerman RW. Screening and selection of sites for CO_2 sequestration based on pressure buildup. International Journal of Greenhouse Gas Control 2009;3(5):577–85.

Mathieson A, Midgely J, Wright I, Saoula N, Ringrose P. In Salah CO_2 storage JIP: CO_2 sequestration monitoring and verification technologies applied at Krechba, Algeria. Energy Procedia 2011;4:3596–603.

Mazzoldi A, Rinaldi AP, Borgia A, Rutqvist J. Induced seismicity within geological carbon sequestration projects: maximum earthquake magnitude and leakage potential. International Journal of Greenhouse Gas Control 2012;10:434–42.

McGarr A, Bekins B, Burkardt N, Dewey J, Earle P, Ellsworth W, Ge S, Hickman S, Holland A, Majer EJ, Rubinstein J, Sheehan A. Coping with earthquakes induced by fluid injection. Science 2015;347(6224):830–1.

Morris JP, Hao Y, Foxall W, McNab W. In Salah CO_2 storage JIP: hydro-mechanical simulations of surface uplift due to CO_2 injection at In Salah. Energy Procedia 2011;4:3269–75.

Myer LR, Daley TM. Elements of a best practices approach to induced seismicity in geologic storage. Energy Procedia 2011;4:3707–13.

Nordbotten JM, Celia MA. Similarity solutions for fluid injection into confined aquifers. Journal of Fluid Mechanics 2006;561:307–27.

Nordbotten JM, Kavetski D, Celia MA, Bachu S. Model for CO_2 leakage including multiple geological layers and multiple leaky wells. Environmental Science and Technology 2009;43(3):743–9.

Pluymakers AMH, Niemeijer AR. Healing and sliding stability of simulated anhydrite fault gouge: effects of water, temperature and CO_2. Tectonophysics 2015;656:111–30.

Pruess K, Oldenburg C, Moridis G. TOUGH2 user's guide, version 2.1, LBNL-43134 (revised). Berkeley, USA: Lawrence Berkeley National Laboratory; 2012.

Rinaldi AP, Rutqvist J. Modeling of deep fracture zone opening and transient ground surface uplift at KB-502 CO_2 injection well, In Salah, Algeria. International Journal of Greenhouse Gas Control 2013;12:155–67.

Rinaldi AP, Rutqvist J, Cappa F. Geomechanical effects on CO_2 leakage through fault zones during large-scale underground injection. International Journal of Greenhouse Gas Control 2014a;20:117–31.

Rinaldi AP, Jeanne P, Rutqvist J, Cappa F, Guglielmi Y. Effects of fault-zone architecture on earthquake magnitude and gas leakage related to CO_2 injection in a multilayered sedimentary system. Greenhouse Gas Science and Technology 2014b;4(1):99–120.

Rinaldi AP, Vilarrasa V, Rutqvist J, Cappa F. Fault reactivation during CO_2 sequestration: effects of well orientation on seismicity and leakage. Greenhouse Gas Sciences and Technology 2015;5(5):645–56.

Ringrose PS, Roberts DM, Gibson-Poole CM, Bond C, Wightman R, Taylor M, Raikes S, Iding M, Østmo S. Characterisation of the Krechba CO_2 storage site: critical elements controlling injection performance. Energy Procedia 2011;4:4672–9.

Ringrose PS, Mathieson AS, Wright IW, Selama F, Hansen O, Bissell R, Saoula N, Midgley J. The In Salah CO_2 storage project: lessons learned and knowledge transfer. Energy Procedia 2013;37:6226–36.

Rutqvist J. Status of the TOUGH-FLAC simulator and recent applications related to coupled fluid flow and crustal deformations. Computers & Geosciences 2011;37(6):739–50.

Rutqvist J. The geomechanics of CO_2 storage in deep sedimentary formations. Geotechnical and Geological Engineering 2012;30(3):525–51.

Rutqvist J, Wu YS, Tsang CF, Bodvarsson G. A modeling approach for analysis of coupled multiphase fluid flow, heat transfer, and deformation in fractured porous rock. International Journal of Rock Mechanics and Mining Sciences 2002;39(4):429–42.

Rutqvist J, Birkholzer J, Cappa F, Tsang CF. Estimating maximum sustainable injection pressure during geological sequestration of CO_2 using coupled fluid flow and geomechanical fault-slip analysis. Energy Conservation and Management 2007;48(6):1798–807.

Rutqvist J, Vasco D, Myer L. Coupled reservoir-geomechanical analysis of CO_2 injection and ground deformations at In Salah, Algeria. International Journal of Greenhouse Gas Control 2010;4:225–30.

Rutqvist J, Liu HH, Vasco DW, Pan L, Kappler K, Majer E. Coupled non-isothermal, multiphase fluid flow, and geomechanical modeling of ground surface deformations and potential for induced micro-seismicity at the In Salah CO_2 storage operation. Energy Procedia 2011;4:3542–9.

Rutqvist J, Cappa F, Rinaldi AP, Godano M. Modeling of induced seismicity and ground vibrations associated with geologic CO_2 storage, and assessing their effects on surface structures and human perception. International Journal of Greenhouse Gas Control 2014;24:64–77.

Segall P, Fitzgerald SD. A note on induced stress changes in hydrocarbon and geothermal reservoirs. Tectonophysics 1998;289(1–3):117–28.

Siskind DE, Stagg MS, Kopp JW, Dowding CH. Structure response and damage produced by ground vibrations from surface blasting. Washington, D.C.: U.S. Bureau of Mines; 1980. Report of Investigations 8507.

Stork AL, Verdon JP, Kendall JM. Assessing the microseismic response at the In Salah carbon capture and storage (CCS) site. International Journal of Greenhouse Gas Control 2015;32:159–71.

Streit JE, Hillis RR. Estimating fault stability and sustainable fluid pressures for underground storage of CO_2 in porous rock. Energy 2004;29(9–10):1445–56.

The National Research Council. Induced seismicity potential in energy technologies. Washington, D.C.: National Academies Press; 2012.

Urpi L, Rinaldi AP, Rutqvist J, Cappa F, Spiers CJ. Dynamic simulation of CO_2-injection-induced fault rupture with 1 slip-rate dependent friction coefficient. Geomechanics for the Energy and Environment 2016;7:47–65.

U.S. Army Corps of Engineers (USACE). Systematic drilling and blasting for surface excavations. Engineering Manual EM1110-2-3800. USACE 1972.

Vasco DW, Rucci A, Ferretti A, Novali F, Bisell R, Ringrose PS, Mathieson AS, Wright IW. Satellite-based measurements of surface deformation reveal fluid flow associated with the geological storage. Geophysical Research Letters 2010;37:L03303. http://dx.doi.org/10.1029/2009GL041544.

Verberne BA, Plümper O, Winter DAM, Spiers CJ. Superplastic nanofibrous slip zones control seismogenic fault friction. Science 2014;346(6215):1342–4.

Verdon JP. Significance for secure CO_2 storage of earthquakes induced by injection. Environmental Research Letters 2014;9(6):064022.

Verdon JP, Stork AL, Bissell RC, Bond CE, Werner MJ. Simulation of seismic events induced by CO_2 injection at In Salah, Algeria. Earth and Planetary Science Letters 2015;426:118–29.

Viegas G, Abercrombie RE, Kim WY. The 2002 M5 Au Sable Forks, NY, earthquake sequence: source scaling relationships and energy budget. Journal of Geophysical Research: Solid Earth 2010;115(B7):B07310. http://dx.doi.org/10.1029/2009JB006799.

Vilarrasa V, Carrera J. Geologic carbon storage is unlikely to trigger large earthquakes and reactivate faults through which CO_2 could leak. Proceedings of the National Academy of Sciences of the United States of America 2015;112(19):5938–43.

Weingarten M, Ge S, Godt JW, Bekins BA, Rubinstein JL. High-rate injection is associated with the increase in U.S. mid-continent seismicity. Science 2015;348(6241):1336–40.

White JA, Chiaramonte L, Ezzedine S, Foxall W, Hao Y, Ramirez A, McNab W. Geomechanical behavior of the reservoir and caprock system at the In Salah CO_2

storage project. Proceedings of the National Academy of Sciences of the United States of America 2014;111(24):8747–52.
Wright I. In Salah CO_2 storage JIP lessons learned. In: Proceedings of the 10th Annual Conference on Carbon Capture and Sequestration. Pittsburgh, Pennsylvania; 2011.
Zhang Y, Person M, Rupp J, Ellett K, Celia MA, Gable CW, Bowen B, Evans J, Bandilla K, Mozley P, Dewers T, Elliot T. Hydrogeologic controls on induced seismicity in crystalline basement rocks due to fluid injection into basal reservoirs. Groundwater 2013;51(4):525–38.
Zoback MD, Gorelick SM. Earthquake triggering and large-scale geologic storage of carbon dioxide. Proceedings of the National Academy of Sciences of the United States of America 2012;109(26):10164–8.
Zoback MD, Zoback ML. Tectonic stress field of the conterminous United States. Geological Society of America Memoirs 1989;172:523–40.

Dr. Jonny Rutqvist is a Senior Scientist at the Lawrence Berkeley National Laboratory (LBNL), Berkeley, California, USA. He holds a PhD degree in engineering geology from the Royal Institute of Technology, Sweden. Rutqvist's research is focused on geomechanics and modeling of coupled thermo-hydro-mechano-chemical (THMC) processes in geological media for a wide range of challenging geoscientific and geoengineering applications, including geologic carbon sequestration, geothermal energy extraction, underground compressed air energy storage, nuclear waste disposal, and unconventional oil and gas resources. Dr. Rutqvist's main contribution to the field of rock mechanics is related to coupled processes model developments and interpretive modeling of large-scale field experiments and data, including complex coupled THM processes associated with some of the largest and longest running heater experiments at underground research laboratories, as well as studies related to geomechanical aspects of reservoir engineering activities such as geothermal energy operations and geologic carbon sequestration. In the early 2000s, Dr. Rutqvist was responsible for the analysis of geomechanics on flow and transport for the previously proposed spent nuclear fuel disposal site at Yucca Mountain Project, Nevada. Also in the early 2000s, Dr. Rutqvist was one of the first to apply coupled geomechanical modeling to geologic carbon sequestration, such as at the In Salah Industry Scale Carbon Sequestration Project in Algeria. At In Salah, Dr. Rutqvist's work on predicting ground surface deformations resulted in a major change in the monitoring strategy of the project, when satellite-based monitoring of ground deformation became the main tool for monitoring the performance of the CO_2 injection operation. Dr. Rutqvist has also made significant contribution to the understanding of coupled THM processes associated with very high temperature geothermal systems, such as at the Geysers Geothermal Field, California. Rutqvist is responsible for modeling support of the Northwest Geysers EGS Demonstration Project, involving stimulation of 1 km^3 reservoir volume by a 1-year injection of "cool" water into a very hot (up to 400 °C), relatively low permeability rock. Dr. Rutqvist's work has in recent years dedicated substantial efforts on modeling of fault activation and induced seismicity associated with underground injection activities, issues that are currently receiving substantial public and media attention. Dr. Rutqvist has also in recent years expanded his coupled processes modeling work to spent nuclear fuel disposal in clay and salt host geological media, as well as deep borehole disposal. The main simulation tool for these studies is the TOUGH-FLAC coupled multiphase fluid flow and geomechanical simulator, which is based on linking the TOUGH2 multiphase fluid flow and heat transport simulator with the FLAC3D geomechanics simulator. Dr. Rutqvist is the principal developer of TOUGH-FLAC at LBNL for 15 years, based on a modeling concept that has been proven very useful and versatile. Dr. Rutqvist has authored over 160 peer-reviewed journal papers and book chapters on the subject, which is cited with an ISI h-index of 32, and is a four-time recipient of the American Rock Mechanics Association (ARMA) Research and Case Study Awards.